Thermal Analysis of a Permanent Magnet Synchronous Motor for Electric Vehicles

Mohamed Amine Fakhfakh [1], Moez Hadj Kasem [2], Souhir Tounsi [3], and Rafik Neji [4]

[1] *Department of Electrical Engineering, University of Sfax, fakhfakhamine@yahoo.fr*
[2] *Department of Electrical Engineering, University of Sfax, kacemm@yahoo.fr*
[3] *Department of Electrical Engineering, University of Sfax, souhir.tounsi@isecs.rnu.tn*
[4] *Department of Electrical Engineering, University of Sfax, rafik.neji@enis.rnu.tn*

Abstract

The thermal issue of electric vehicles is an important criterion for the design of the motor and for choosing the adequate cooling system to assure propels electrical performance and reliability. The thermal behavior of motor depends on the heat sources and on the motor geometry. This paper presents the thermal analysis of permanent magnet synchronous motor (PMSM) for electric vehicles traction application. The thermal design technique used is the analytical lumped circuit. An analytical copper and iron loss model is presented also two cooling systems are applied to this model, cooling by air and water. A comparison is carried out so choosing the best solution. The equivalent circuit of the motor is implemented and simulated with MATLAB simulator. The results obtained show the effectiveness of the designed motor and its good satisfaction of the specification book.

Keywords

thermal analysis, axial flux, permanent magnet synchronous motor, cooling system

1. INTRODUCTION

The thermal management of the motor in an electric vehicle is important because the electrical insulation has a temperature limit, and also because the temperature of the motor affects its efficiency. An accurate simulation of the thermal behaviour of the motor within the power train is therefore an important aspect of designing an appropriate cooling system and strategy [Erik et al., 2005].

The heat sources in a motor are: copper losses and iron losses. The most significant of these is the cooper losses from ohmic resistance and eddy currents. Ohmic resistance losses depend on the current in the coils, while eddy current copper losses depend on motor rpm. Iron losses from eddy currents and hysteresis depend on the rpm. Mechanical losses from windage and bearing friction depend on the rpm.

In this paper we present first the geometry of Permanent Magnet Synchronous Motor (PMSM) studied and losses model of the traction chain strongly parameterized is developed and established under MATLAB/SIMULINK environment.

Second, we present the lumped circuit thermal model used in this study and the two cooling systems used to cool the motor. The lumped circuit approach has a clear advantage over numerical techniques such as Finite Eelements Analysis (FEA) and Computational Fluid Dynamics (CFD) techniques in terms of calculation speed.

2. GEOMETRY STUDIED

Figure 1 shows the geometry of the PMSM design used in this study. The design is a permanent magnet, concentrated winding, opened slot, axial flux and sinusoidal wave-form.

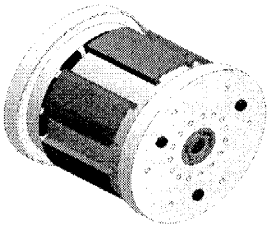

Fig. 1 Studied geometry of PMSM

Figure 2 shows the geometry of the stator and the rotor of PMSM.

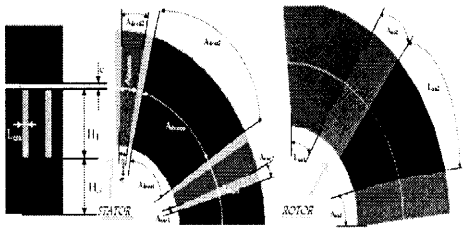

Fig. 2 Stator and rotor geometry

The various characters of PMSM are presented by Table 1.

Table 1 PMSM parameters

Pairs pole number	n	4
Air-gap thickness	e	0.002 m
Principal teeth number	N_{te}	6
stator yoke height	H_{cs}	0.035 m
Outer diameter of stator	$D_{ext.s}$	0.250 m
Inner diameter of stator	$D_{int.s}$	0.150 m
Slot width	L_{enc}	0.005 m
Lower slot angular	$Aenc_1$	4°
Higher slot angular	$Aaenc_2$	2.4°
Lower angular of principal tooth	$Adent_1$	44°
Higher angular of principal tooth	$Adent_2$	45.6°
Lower angular of inserted tooth	$Adenti_1$	8°
Higher angular of inserted tooth	$Adenti_2$	9.6°
Slot height	H_d	0.144 m
Outer diameter of rotor	$D_{ext.r}$	0.250 m
Inner diameter of rotor	$D_{int.r}$	0.150 m
Rotor yoke height	H_{cr}	0.026 m
Magnet height	H_a	0.0067 m
Magnet section	S_a	0.0026 m^2

From physical property of material and the motor geometry we can deduce the different analytical dimensioning equations.
The magnet height is given by:

$$H_a = \frac{\mu_r B_e e}{B_r - \frac{B_e}{K_{fu}}} \quad (1)$$

Where:
μ_r: magnets relative permeability
Be: air-gap magnetic induction
e: air-gap thickness
Br: magnets remanent magnetic induction
Kfu: flow escapes coefficient
*The height of teeth is given by:

$$H_d = \frac{3N_{sph}I_d}{N_t \delta K_f L_{enc}} \quad (2)$$

Where:
N_t: number of principal teeth
I_d: motor rated current
K_r: slot load factor
N_{sph}: number of spire by phase
L_{enc}: width of the notches
ä:density of the acceptable current in copper

* The rotor yoke thickness is given by:

$$H_{cr} = \frac{B_e}{B_{cr}} \mathrm{Min} \frac{(S_d, S_a)}{(D_{ext} - D_{int})} \frac{1}{K_{fu}} \quad (3)$$

Where:
Dext: outer diameter of motor
Dint: inner diameter of motor
Sd: teeth section
Sa: magnet section
Bcr: magnetic induction of rotor yoke
* The stator yoke thickness is given by:

$$H_{cs} = \frac{B_e}{B_{cs}} \mathrm{Min} \frac{(S_d, S_a)}{(D_{ext} - D_{int})} \quad (4)$$

Where:
Bcs: stator yoke magnetic induction
B_e: air-gap magnetic induction
The electromagnetic torque is given by the following equation [Tounsi and al., 2004].

$$C_{em} = \frac{3EI}{2\Omega} \quad (5)$$

With:
Ù : angular velocity
I: phase current
E: electromotive force
*The motor electric constant
The motor electric constant Ke is calculated so that the electric vehicle can function at speed stabilized with a weak undulation of the couple.

$$K_e = \frac{3}{2} N_{sph} \frac{(D_{ext}^2 - D_{int}^2)}{4} B_e \quad (6)$$

*The electromotive force
The electromotive force E is deduced from the analytical model, it is given by the following relation:

$$E = 2N_{sph}\Omega \frac{(D_{ext}^2 - D_{int}^2)}{8} Be \quad (7)$$

$$\Rightarrow E = \frac{2}{3}\Omega K_e \quad (8)$$

* Electromagnetic torque
We can deduce from the equations (5), (6) and (8) the expression of the couple:

$$C_{em} = K_e I \quad (9)$$

3. LOSSES MODELING

3.1 Copper losses

In a synchronous permanent magnet machine, the copper losses are function by phase current and phase resis-

tance [GASC L, 2004]. The copper losses are given by the following expression:

$$Pj = 3R_{ph}I_{eff}^2 = 3R_{ph}\left(\frac{i_{max}}{\sqrt{2}}\right)^2 \quad (10)$$

R_{ph} is the phase resistance given by the following expression:

$$R_{ph} = R_{cu}(T_{cu})\frac{N_{sph}L_{sp}}{S_c} \quad (11)$$

With:
Tcu: copper temperature
Lsp: spire average length
Sc: spire section

3.2 Iron losses

The iron losses are described as losses in the stator yoke and teeth [Pertusa, 1996].
* The iron losses in the teeth are given by:

$$P_{f\_d} = q\left(\frac{f}{50}\right)^{1.5}\left[M_{ds}B_d^2\right] \quad (12)$$

Where:
q: quality coefficient of the meta sheets
f: supply frequency of the motor
B_d: peak flux density value in the teeth
M_{ds}: teeth mass
* The iron losses in the stator yoke are given by:

$$P_{f\_c} = q\left(\frac{f}{50}\right)^{1.5}\left[M_{cs}B_{cs}^2\right] \quad (13)$$

Where:
B_d: peak flux density value in the stator yoke

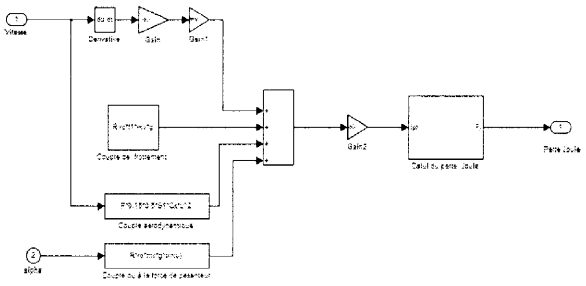

Fig. 3 Model of copper losses

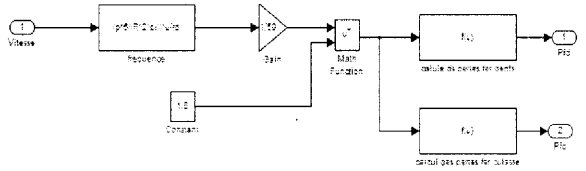

Fig. 4 Model of iron losses

M_{ds}: stator yoke mass
The Figure 3 and Figure 4 describe respectively the model of the copper losses and the iron losses implemented under MATLAB SIMULINK environment.

4. LUMPED CIRCUIT ANALYSIS

The thermal model is based upon lumped-circuit analysis. It represents the thermal problems by using the thermal networks, analogous to electrical circuits. The thermal circuit in the steady state consists of thermal resistances and heat sources connected between motor component nodes [Chin et al., 2003; Staton, 2001; Staton et al., 2003]. For transient analysis, the heat/thermal capacitances are used additionally to take into account the change in internal energy of the body with time. Thermal resistances for conduction and convection can be obtained by:

$$R_{conduction} = \frac{l}{A.k}[K/W] \quad (14)$$

$$R_{convection} = \frac{1}{A_c h}[K/W] \quad (15)$$

Where l is the distance between the point masses and A is the interface area, k is the heat conductivity, Ac is the cooling cross section between the two regions and h is the convection coefficient – calculated from proven empirical dimensionless analysis algorithms [Holman, 1992]. The heat capacitance is defined as:

$$C = V.\rho c \text{ [Ws/K]} \quad (16)$$

Where V is the volume, $\tilde{n}$ is the density and c is the heat capacity of the material. Figure 5 presents the schematic diagram of a transient state thermal network of a PMSM.
As described earlier, the thermal resistance values are automatically calculated from motor dimensions and material data. The accuracy of the calculation is dependent on knowledge of the various thermal contact resistances between components within the motor, e.g. slot-liner to lamination and lamination to housing interface. Figure 5 shows a longitudinal section of the motor for

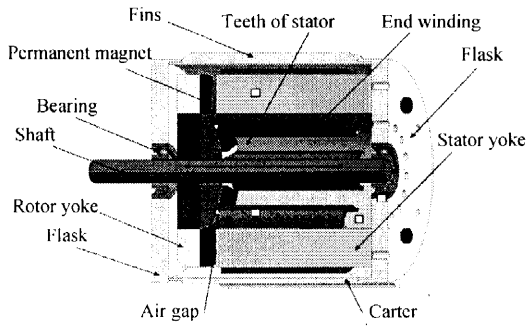

Fig. 5 Longitudinal section of the motor

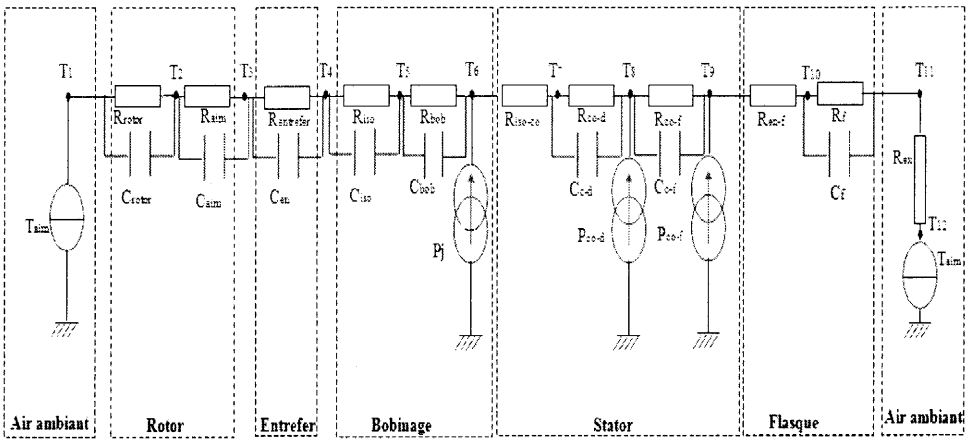

Fig. 6 Transient thermal model

thermal study. The thermal resistances are calculated along the axial direction. The Ri radius are calculated from dimensions of motor.

The transient thermal model is shown in Figure 6. The sources of heat in this model correspond respectively to the copper losses and iron losses in the stator.

The variables Ti correspond to the temperatures in various points of the motor. The expressions of thermal resistances result from the resolution of the equation of heat at the borders of the fields.

In this model, ten main heat conductions exist in the motor. Rrotor represents the conduction resistance of the rotor iron; Raim represents the conduction resistance of the magnet; Rentrefer represents conduction resistance air-gap; Riso represents the conduction resistance of isolating; Rbob represents the conduction resistance of copper; Riso-co represents the conduction resistance between isolating and stator yoke; Rco-d represents the conduction resistance of teeth; Rco-f represents the conduction resistance of stator yoke; Ren-f represents the conduction resistance between the stator yoke and the aluminium back plate and Rf represents the conduction resistance of aluminium back plate. Rex represents the convection resistance between the motor and the air.

In this equivalent thermal network model, "C_{rotor}", "C_{aim}", "C_{en}", "C_{iso}", "C_{bob}", "$C_{c\text{-}d}$", "$C_{c\text{-}f}$" and "C_f" represent the thermal capacity of the iron rotor, magnet, air-gap, isolating, copper wire, teeth, stator yoke and aluminium back plate.

5. SIMULATION WITHOUT COOLING SYSTEM

We fixed at 120°C the maximum winding temperature and at 50°C the limit temperature of magnet. For intermittent operation a mission of circulation is used. Figure 7 represents the mission of circulation used for the simulation of the thermal behavior of our model.

From this mission we deduce the coppers losses and iron losses injected into thermal model presented by Figure 8.

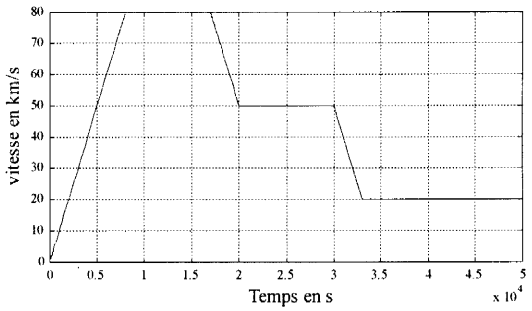

Fig. 7 Mission of circulation

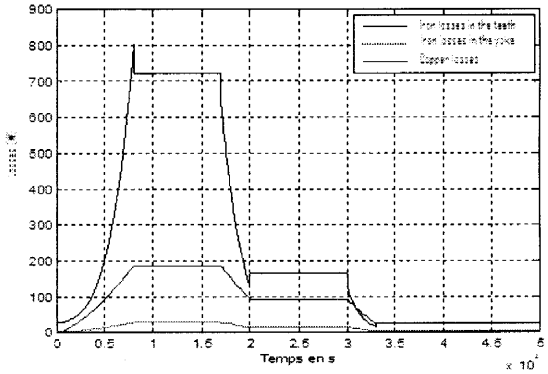

Fig. 8 Losses

The different temperatures at any part of the motor are shown from Figure 9 to Figure 14.

Figure 15 shows the motor temperature at 80 km/h for continuous operation. The winding temperature is higher than 120°C, so a cooling system is necessary to used.

6. COOLING SYSTEMS AND RESULTS

All the losses described result in a heating which must be evacuated. Certain materials such as isolating and copper are sensitive to heat. It is thus necessary to transport this heat towards a cooling system: it is the object

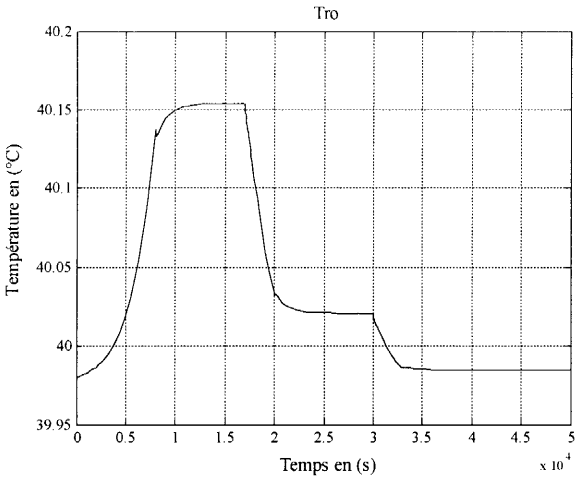

Fig. 9 Rotor temperature

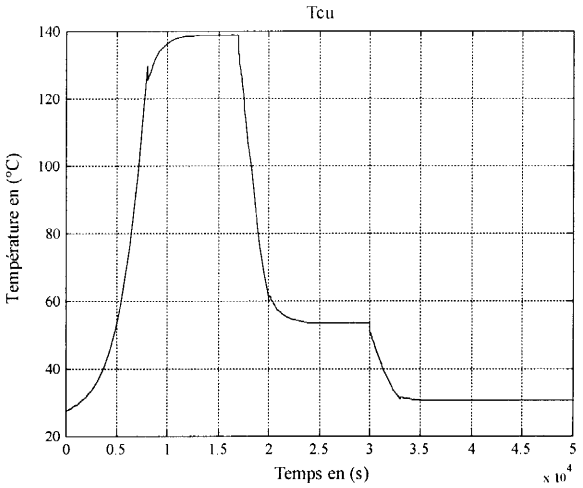

Fig. 12 Winding temperature

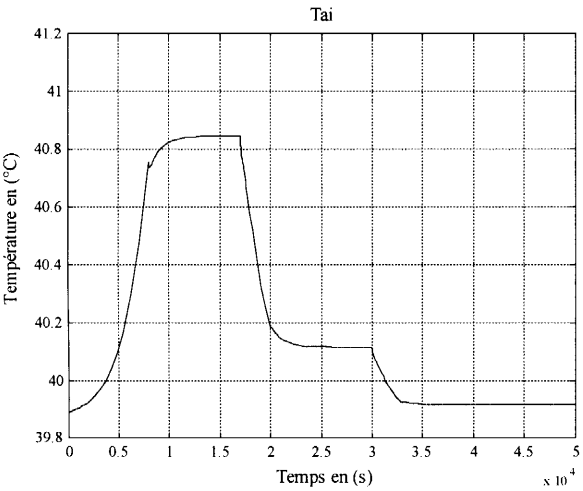

Fig. 10 Magnet temperature

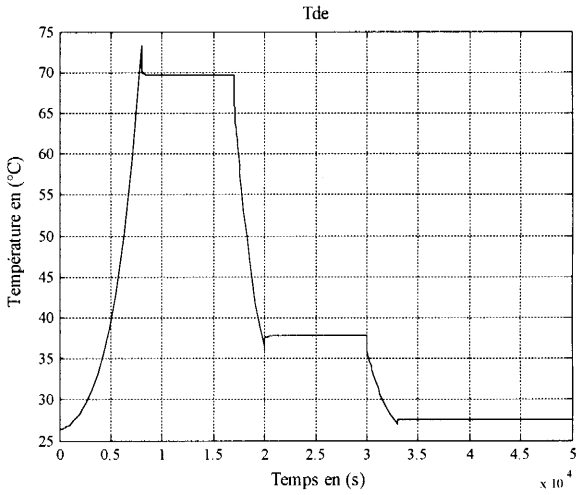

Fig. 13 Teeth temperature

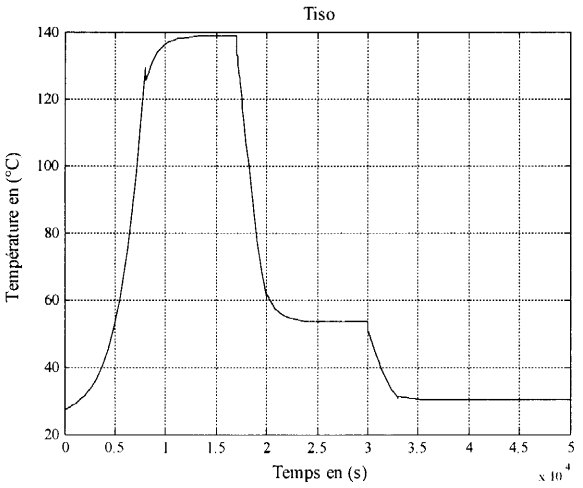

Fig. 11 Isolating temperature

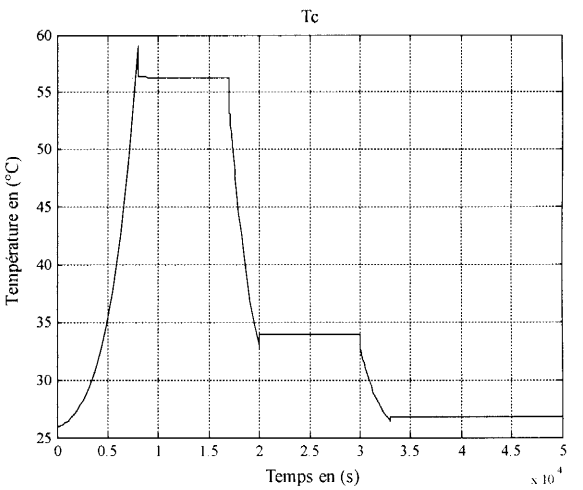

Fig. 14 Stator yoke temperature

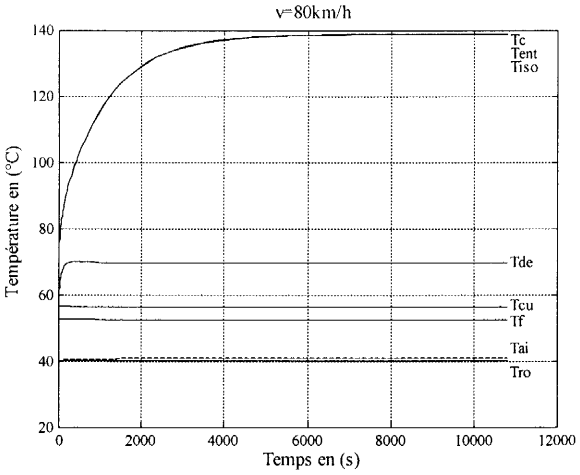

Fig. 15 Motor temperature at 80km/h

of standard CEI 34-6 [Coudert et al., 1988].

The fluids used for the transport of heat are usually air, water or oil and more rarely carbon dioxide, nitrogen or hydrogen. In our study we use cooling by fins and water cooling. Figure 16 shows the PMSM with cooling fins.

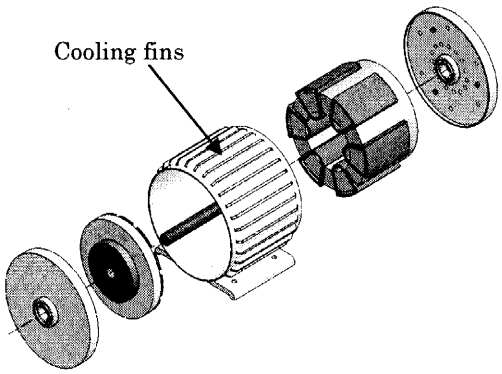

Fig. 16 PMSM with cooling fins

We can with a constant heat flux decrease the temperature of a wall or with a constant temperature increase the flux which is exchanged with its environment. These fins, which penetrate in the fluid in a direction OX on a depth L, can be with uniform section or not (Figure 17).

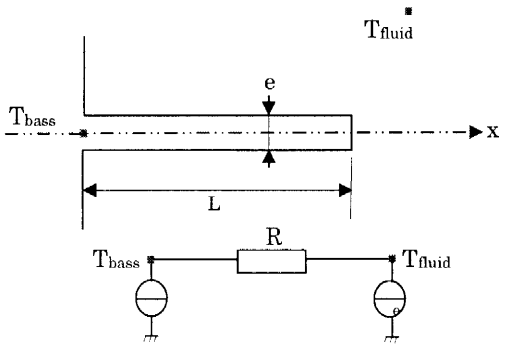

Fig. 17 Cooling fins, diagram and thermal resistance

The heat differential equation of fins is given by the following equation [Glises, 1998]:

$$S\frac{d^2T(x)}{dx^2} + \frac{hP}{\lambda}T(x) = 0 \qquad (17)$$

Where:

P: perimeter of the fins section

S: fins section

h: convection coefficient

ë: thermal conductivity of aluminum

The boundary conditions necessary to its integration are:

- For $X = 0$, $T = Tbase$
- For $X = L$, $T = Tfluide$

We consider practically that the heat flux exchanged at the end of the fins is negligible. The integration of the equation (17) gives:

$$\frac{T - T_{fluide}}{T_{base} - T_{fluide}} = \frac{\cosh(m(L-x))}{\cosh(mL)} \qquad (18)$$

With:

$$m = \sqrt{\frac{h.P}{\lambda.S}} \qquad (19)$$

Thus, the thermal conduction resistance between fins and air is given by:

$$R_a = \frac{1}{\sqrt{h.P.\lambda.S}\tanh(m.L)} \qquad (20)$$

Figure 18 shows the motor temperature at 80km/h using the cooling fins. The motor temperature was decreased but the winding temperature is higher than 120°C.

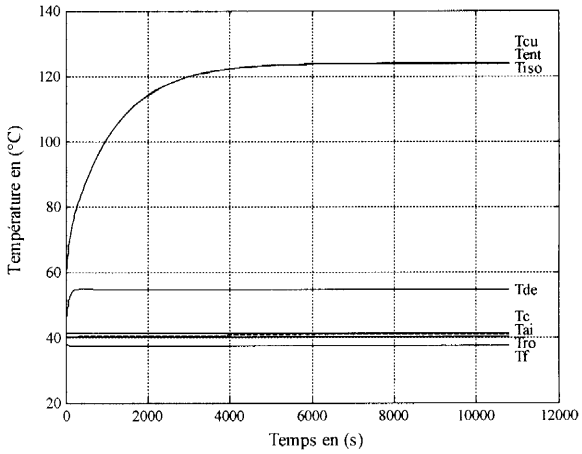

Fig. 18 Motor temperature with cooling fins at 80km/h

Water cooling is very efficacy than air cooling. It dissipates more power with a lower flow. Water is approximately 1000 times denser than air and is able to store a much quantity of heat per unit of mass. The details of the physical properties of air and water can be found in

Table 2 Physical property

Fluid	Specific heat	Density
Water	4217J/kg·°C	998kg/m³
Air	1060J/kg·°C	1.2 kg/m³

the table below:

Figure 19 shows the motor temperature at 80km/h with water cooling. It is clear that the temperature has decreased and in particularly the winding temperature is less than 120°C. Figure 20 shows the winding temperature with and without cooling system at 80km/h.

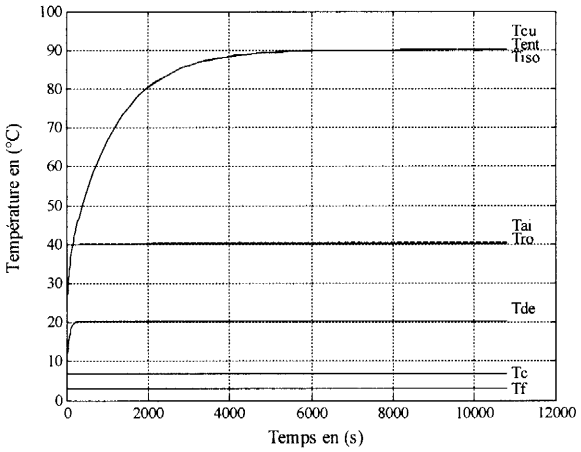

Fig. 19 Motor temperature with water cooling at 80km/h

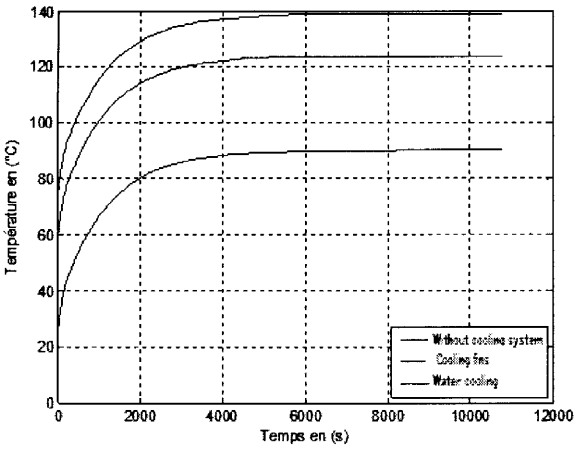

Fig. 20 Copper temperature at 80km/h

7. CONCLUSION

The thermal analysis of an axial flux permanent magnet synchronous motor for electric vehicle traction application fixed by the specification book is presented. The lumped circuit approach is employed in this investigation. In this paper two different cooling systems are presented and investigated. The motor temperatures at continuous and intermitted operation are also presented. From the results, it is clear that the water cooling is also the better solution to cooling our motor and to satisfy the fixed book qualifications.

References

Chin Y. K., E. Nordlund, and E. A. Staton, Thermal analysis: Lumped circuit model and finite element analysis, *Sixth International Power Engineering Conference (IPEC)*, 952-957, 2003.

Nordlund, E., S. Tsakok, A. Walker, P. Anpalahan, and M. Lampérth, Lumped Circuit Thermal Model of an Axial Flux Motor, *The 21st Worldwide Battery, Hybrid and Fuel Cell Electric Vehicle Symposium and Exhibition*, 2005.

GASC L, Conception d'un actionneur à aimants permanents à faible ondulation de couple pour assistance de direction automobile: Approche par la structure et la commande, Thèse de doctorat, *Institut National Polytechnique de TOULOUSE*, 2004.

Holman J. P., *Heat Transfer*, Seventh Edition, McGraw-Hill Publication, 1992.

Coudert, J. L., P. Delsalle, C. Dupuis et D. Hottois, Construction mécanique des machines électriques tournantes: Considérations générales, *Techniques de l'ingénieur*, Vol. D3III, No. D3780, 1-23, 1988.

Pertusa, Contribution à la définition de moteurs à aimants permanents pour un véhicule électrique hybride routier, *Thèse de l'Institut National Polytechnique de Toulouse*, 1996.

Glises, R., Machines électriques tournantes Simulation du comportement thermique, *Techniques de l'ingénieur D3760*, 1998.

Staton, D. A., A. Boglietti, and A. Cavagnino, Solving the More Difficult Aspects of Electric Motor Thermal Analysis, *IEEE IEMDC 2003 Conference Proceedings*, 2003.

Staton, D. A., Thermal analysis of electric motors and generators, *Tutorial course at IEEE IAS Annual Meeting*, 2001.

Tounsi S, R. Neji, F. Sellami, Modélisation des Pertes dans la Chaîne de Traction d'un Véhicule Electrique, *Conférence Tunisienne de Génie Electrique*, 2004.

(Received August 22, 2008; accepted October 14, 2008)